

## Research Article

## Health risk assessment of Fluoride and Cadmium enrichment in rural drinking groundwater in Shanxi Province, China

Qi-fa Sun<sup>1,2,3,4</sup>, Bing Lu<sup>1,2\*</sup>, Chuan-lei Lu<sup>1,2\*</sup>, Yuan Yang<sup>1</sup>, Xu Xie<sup>1</sup>, Lin Guo<sup>1,3</sup>, Chen Hu<sup>1,3</sup>, Xu Wang<sup>1,3</sup><sup>1</sup> Harbin Center for Integrated Natural Resources Survey, China Geological Survey, Harbin 150086, China.<sup>2</sup> Observation and Research Station of Earth Critical Zone in Black Soil, Ministry of Natural Resources, Harbin 150086, China.<sup>3</sup> Northeast Geological Science and Technology Innovation Center, China Geological Survey, Shenyang 110034, China.<sup>4</sup> Key Laboratory of Groundwater Resources Development and Protection in the Songnen-Sanjiang Plain of Heilongjiang Province, Harbin 150086, China.

**Abstract:** Excessive levels of Fluoride (F<sup>-</sup>) and Cadmium (Cd) in drinking groundwater may pose health risks. This study assessed the health risks associated with F<sup>-</sup> and Cd contamination in rural drinking groundwater sources in Wutai County, Shanxi Province, China, to support population health protection, water resource management, and environmental decision-making. Groundwater samples were collected and analyzed, and a Human Health Risk Model (HHRA) was applied to evaluate groundwater quality. The results showed that both contents of F<sup>-</sup> and Cd in groundwater exceeded the Class III limits of China's national groundwater quality standard (GB/T 14848—2024). Fluoride levels met the Class V threshold, with enrichment area mainly located in the east part of the study area. Cadmium levels reached Class IV, with elevated concentrations primarily observed in the western and northwestern regions. Correlation analysis revealed that F<sup>-</sup> showed weak or no correlation with other measured substances, indicating independent sources. Health risk assessment results indicated that F<sup>-</sup> poses potential health risks to rural residents, while cadmium, due to its relatively low concentrations, does not currently present a significant health risk. Among different demographic groups, the health risk levels of F<sup>-</sup> exposure followed the order: Infants > children > adult females > adult males. The findings highlight that fluoride is the primary contributor to health risks associated with groundwater consumption in the study area. Strengthened monitoring and prevention of F<sup>-</sup> contamination are urgently needed. This research provides a scientific basis for the prevention and control of fluoride pollution in groundwater and offers practical guidance for safeguarding drinking water safety in rural China.

**Keywords:** Rural China; Groundwater quality; Fluoride; Cadmium; Source analysis; Health risk assessment

Received: 12 Nov 2024/ Accepted: 30 Jun 2025/ Published: 20 Nov 2025

## Introduction

Long term consumption of groundwater enriched with fluoride (F<sup>-</sup>) and cadmium (Cd) poses poten-

tial health risks. Fluoride is an essential trace element for the human body; small amounts are beneficial, particularly in preventing osteoporosis. However, excessive intake can lead to adverse health effects, mainly manifesting as dental and skeletal fluorosis (Sun et al. 2023a). Cadmium, on the other hand, is a non-essential and toxic element. Once released into the environment, it can bioaccumulate and enter the human body through the food chain, potentially leading to chronic poisoning (Sanjay et al. 2024). Understanding the classification and distribution of hazardous substances in groundwater, along with a scientific assessment of their associated health risks, is criti-

\*Corresponding author: Bing Lu, Chuan-lei Lu, E-mail address: 2208408367@qq.com, 819070179@qq.com

DOI: 10.26599/JGSE.2026.9280067

Sun QF, Lu B, Lu CL, et al. 2026. Health risk assessment of Fluoride and Cadmium enrichment in rural drinking groundwater in Shanxi Province, China. Journal of Groundwater Science and Engineering, 14(1): 1-14.

2305-7068/© 2026 Journal of Groundwater Science and Engineering Editorial Office This is an open access article under the CC BY-NC-ND license (<http://creativecommons.org/licenses/by-nc-nd/4.0>)

cal for effective prevention and control, ensuring the daily safety of drinking water for rural populations.

Churchill et al. (1948) were among the first to report that mining activities could contribute to groundwater fluoride enrichment, sparking interest in the link between anthropogenic activities and fluoride contamination. In China, research on fluoride in groundwater began in the 1980s. Li et al. (1980) identified hydrochemical types, meteorological conditions, and hydrogeology as key factors influencing fluoride concentrations. More recent studies have expanded the understanding of fluoride enrichment mechanisms. For instance, Xiao et al. (2015) and Li et al. (2021) analyzed the spatial distribution and genesis of high-fluoride groundwater in the central Loess Plateau and northern Lingwu City, respectively, and concluded that geological background, topography, climate, and human activities are the main factors. Similarly, Cao et al. (2023a) explored the spatial distribution and controlling mechanisms of high-fluoride groundwater in the Bohai coastal plain. Building on this, Cao et al. (2024) applied enhanced superposition learning model to predict fluoride levels in groundwater across the North China Plain, advancing research from spatial characterization to predictive modelling.

In contrast, cadmium pollution in groundwater has attracted less global attention, as it is not universally widespread. Marghade et al. (2021) assessed the pollution levels of untreated wastewater and heavy metal in the Euphrates River, which flows through Türkiye, Syria and Iraq, and found cadmium concentrations exceeding Iraq's national standards. In another study, José et al. (2021) monitored Cd concentrations in agricultural groundwater in the Mororito River Basin in Mexico and concluded that the average Cd level was within national and international drinking water guidelines. These findings suggest that Cd pollution in groundwater is regionally specific rather than a globally prevalent issue.

To ensure the safety drinking water, it is essential to study the sources of heavy metal contamination in groundwater. Hu et al. (2024) analyzed the characteristics and sources of heavy metal pollution in groundwater from coal-mining-intensive areas and identified four main sources: Industrial emissions, coal gangue leaching, geological factors, and emissions from gas stations and from breeding. Of these, industrial discharge and coal gangue leaching were the most significant. Additionally, Cao et al. (2023b) conducted a stacking ensemble learning modeling to map the potential

heavy metal enrichment and distribution in the lower Yellow River plain, providing further insight into their regional occurrence patterns.

Groundwater is an important natural resource, and ensuring its quality is crucial for safeguarding public health. To regulate groundwater quality, China has established the *Sanitary Standards for Drinking Water* (GB 5749—2022) and the *Groundwater Quality Standards* (GB/T 14848—2024), which stipulate that the concentrations of  $F^-$  and Cd in centralized drinking water sources must not exceed 1.0 mg/L and 0.005 mg/L, respectively.

Groundwater health risk assessment is an effective method for quantitatively evaluating the degree of harm posed by hazardous substances to human health (Nitika, 2021). This process typically involves hazard identification, dose-response analysis, exposure assessment, and risk characterization (Alireza et al. 2020). In this study, hazard assessment was conducted through field investigations, groundwater sampling, and laboratory analysis. Using information from the International Agency for Research on Cancer (IARC), the dose-response relationship for  $F^-$  and Cd exposure were determined (Sun et al. 2023b). Based on the specific environmental and demographic conditions of the study area, relevant indicators were selected to ensure the practical applicability of the assessment, enhancing its regional relevance and policy value (Chen et al. 2017).

To date, the enrichment levels and spatial distribution of  $F^-$  and Cd in groundwater have not been systematically studied in the Gengzhen area of Shanxi Province. To address this gap, this study takes Gengzhen and its surrounding rural area as the research focus. By conducting systematic field surveys, sampling, testing, and spatial analysis, the enrichment characteristics and distribution patterns of  $F^-$  and Cd in groundwater were investigated. The results revealed that the fluoride concentrations in groundwater samples from the study area exceeded the groundwater quality standards, warranting a comprehensive health risk assessment.

Various models have been developed to assess the health risks associated with groundwater contaminants, among which the Human Health Risk Assessment (HHRA) model recommended by the United States Environmental Protection Agency (USEPA) is the most widely adopted (Sun et al. 2020a; Sun et al. 2020b; Anju et al. 2022; Sun et al. 2024b). Based on the HHRA framework and in consideration of the local hydrogeological and socio-economic context, a tailored health risk assessment model was established to scientifically

evaluate the health risks of  $F^-$  and  $Cd$  in the groundwater of Gengzhen and surrounding areas. The findings not only contribute to ensuring safe and healthy drinking water in Shanxi Province, but also provide a methodological reference for conducting groundwater health risk assessments in similar rural regions.

## 1 Materials and methods

### 1.1 Study area

The study area is located in Gengzhen Town and surrounding areas within Wutai County, situated in the central eastern part of Shanxi Province in China, with geographical coordinates spanning from  $113^\circ 15' 30''$  to  $113^\circ 45' E$  and from  $38^\circ 40'$  to  $38^\circ 50' N$ . The area experiences a typical continental monsoon climate, suitable for cultivating crops such as corn, millet, oilseeds, naked oats, beans, potatoes and etc. Geomorphologically, the region consists of mid-mountain terrain characterized by rivers and valleys, with an overall elevation gradient descending from north to south. The exposed strata include those from the Precambrian, Proterozoic, Paleozoic, and Cenozoic eras, with the Quaternary loose layer mainly composed of loess. The geological structure of the area lies within the Lvliang-Taihang fault block zone. Groundwater is primarily recharged by atmospheric precipitation. The main surface water body is Qingshui River, which flows from northeast to southwest, exhibiting a

discharge pattern consistent with that of regional groundwater. There are three types of aquifers in the area: Loose rock pore aquifer, carbonate rock karst-fracture aquifer, and metamorphic fractured rock aquifer. Groundwater levels in the loose and metamorphic rock aquifers are relatively shallow, while carbonate rock aquifer is more deeply buried. The lithology in the area includes granite, basalt, syenite, gneiss, ultramafic rocks, amphibolite, dolomite, marble, schist, slate, phyllite, quartzite, sandstone, and various carbonate rocks.

### 1.2 Sampling and measurements

Groundwater samples were systematically collected across the study area in June 2024; and the selected samples represent the Quaternary aquifer which is the primary water source for local residents. A total of 29 groundwater samples were obtained, with sampling sites evenly distributed throughout the region (Fig. 1). Samples collection, storage, and transport strictly followed the *Technical Specification for Groundwater Environmental Monitoring* (H/164-2004). Water quality parameters measured include Total Dissolved Solids (TDS), total hardness (as  $CaCO_3$ ),  $NO_3^-$ , pH,  $Ca^{2+}$ ,  $Mg^{2+}$ ,  $K^+$ ,  $Na^+$ ,  $Cl^-$ ,  $SO_4^{2-}$ ,  $HCO_3^-$ . All water sample analyses were conducted by the Harbin Comprehensive Survey Center for Natural Resources, China Geological Survey, with analytical methods including: Gravimetric method for TDS, titration for  $CaCO_3$  and  $HCO_3^-$ , ion chromatography for  $NO_3^-$ ,  $K^+$ ,  $Na^+$ ,  $Cl^-$ , and  $SO_4^{2-}$ , glass electrode

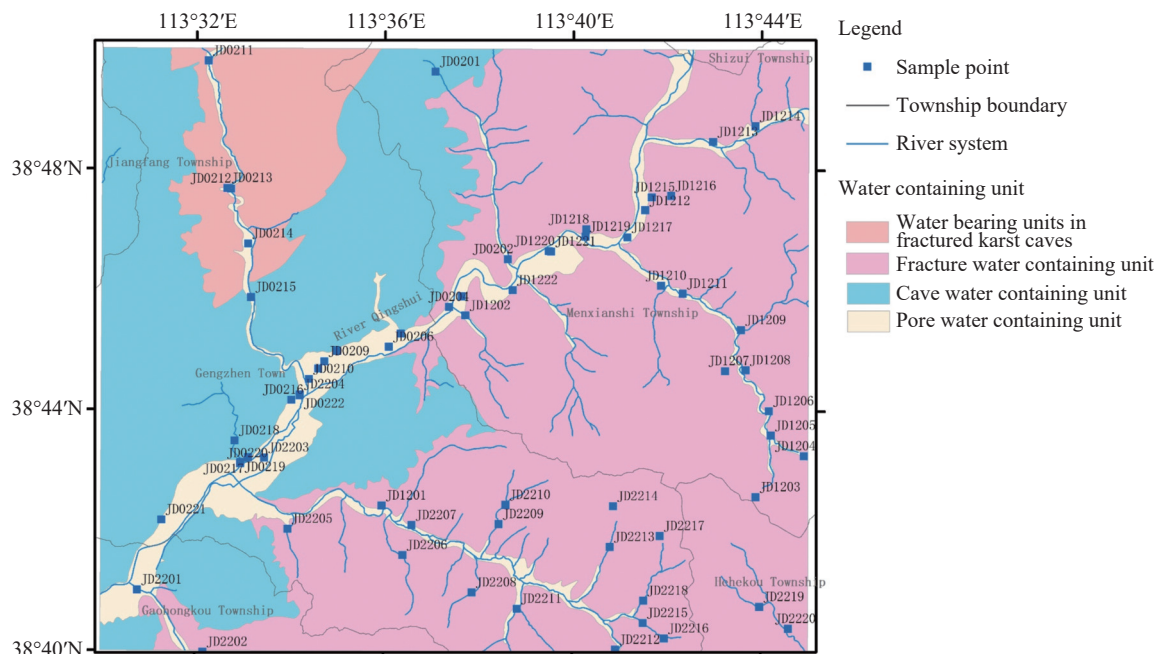


**Fig. 1** Spatial distribution of groundwater sampling sites in the study area

method for pH, and EDTA titration for  $Mg^{2+}$  and  $Ca^{2+}$ . A summary of the analytical methods and associated detection limits for each parameter is detailed in Table 1.

To ensure data quality, an anion-cation balance check was performed. Only data with a relative error (E) less than 5% were considered reliable; and all samples passed this criterion. Additionally, data precision was assessed by duplicate sample analysis, with relative deviation rates exceeding 90% across all sample batches, indicating high analytical reliability.

### 1.3 Human health risk assessment model and parameter acquisition

#### Hazard identification

The first step in the Human Health Risk Assess-

ment (HHRA) is hazards identification which aims to determine the potential adverse effects of human exposure to hazardous substances, the likelihood of such effects occurring, and the associated uncertainties. The objective is to evaluate the weight of evidence for health risks based on toxicological data and mode-of-action studies (Sun et al. 2024a; Saravanan et al. 2022).

To achieve this, detailed site-specific information is required, including historical and current pollutant concentration data in groundwater, physicochemical properties of the site, climate, site hydrological and geological information, land use patterns, population vulnerability, and distribution of sensitive receptors.

#### Dose-response assessment

According to the four step HHRA framework established by the USEPA, the dose-response

**Table 1** Analytical methods and detection limits for groundwater quality parameters

Analyte	Analytical method	Detection limit (mg/L)
$Na^+$	Ion chromatography	1
$Ca^{2+}$	Acidic permanganate titrimetric method	4
$Mg^{2+}$	Acidic permanganate titrimetric method	3
$NH_4^+$	Ion chromatography	0.05
$Cl^-$	Ion chromatography	3
$SO_4^{2-}$	Ion chromatography	3
$NO_3^-$	Ion chromatography	0.01
$NO_2^-$	Spectrophotometry	0.010
$F^-$	Ion chromatography	0.05
Cu	Flame atomic absorption spectrophotometry	0.007
Zn	Flame atomic absorption spectrophotometry	0.003
Cd	Flame atomic absorption spectrophotometry	0.007
Ni	Flame atomic absorption spectrophotometry	0.012
$Cr^{6+}$	Catalytic polarographic method	0.02
T Fe	Inductively coupled plasma atomic emission spectrometry	0.05
Mn	Inductively coupled plasma atomic emission spectrometry	0.05
$H_2SiO_3$	Silicon molybdenum yellow spectrophotometry	1.3
As	Hydride generation atomic fluorescence spectrometry	0.0005
Hg	Cold atomic absorption spectrophotometry	0.0001
$COD_{Mn}$	Acidic permanganate titrimetric method	0.4
$CaCO_3$	EDTA titrimetric method	5
TDS	Gravimetric method	—
pH	Glass-electrodes method	—
Sr	Inductively coupled plasma atomic emission spectrometry	0.05
Se	Catalytic polarographic method	0.0005
Li	Ion chromatography	0.02
Al	Inductively coupled plasma atomic emission spectrometry	0.005
Pb	Inductively coupled plasma atomic emission spectrometry	0.3

Note: “—” indicates no applicable detection limit for the parameter.

assessment describes the likelihood and severity of adverse health effects under specific exposure conditions to a chemical substance. It provides a mathematical foundation to convert exposure levels into estimated health risk. The relationship is typically expressed using the reference dose (*RfD*) (Tian et al. 2020b; Tian et al. 2020d), calculated as:

$$RfD = \frac{NOAEL(LOCAEL)}{UFs} \quad (1)$$

Where: *RfD*: Chronic reference dose (mg/kg/d), *LOCAEL*: Lowest observed adverse effect level (mg/kg/d), *NOAEL*: No observed adverse effect level (mg/kg/d), and *UFs*: Uncertainty factors.

For this study:

The groundwater standard for fluoride ( $F^-$ ) is 1.0 mg/L; the *RfD* for oral ingestion is 0.06 mg/kg/d, and for dermal exposure, it is 0.03 mg/kg/d.

The standard for Cadmium (Cd) is 0.005 mg/L; the *RfD* for oral ingestion is 0.001 mg/kg/d, and for dermal exposure, it is 0.0005 mg/kg/d (USEPA, 2001).

#### Exposure assessment

Exposure assessment quantifies the intensity, duration, and frequency of human exposure to pollutants in the environment. It is the quantitative basis for risk assessment and includes assessment of exposure scenarios, concentrations, pathways, and receptors.

According to USEPA guidelines, exposure to groundwater contaminants occurs via three pathways: Ingestion, dermal contact, and inhalation. Since the  $F^-$  and Cd are non-volatile and does not

pose significant inhalation risks, only ingestion and dermal absorption are considered in this study. The exposure doses are calculated using the following equations:

$$I_{CDI} = \frac{C \times IR \times ABS \times EF \times ED}{BW \times AT} \quad (2)$$

$$I_{CDD} = \frac{C \times SA \times K_p \times EV \times ET \times EF \times ED \times CF}{BW \times AT} \quad (3)$$

Where:

*I<sub>CDI</sub>* - Chronic daily intake through ingestion (mg/kg/d).

*I<sub>CDD</sub>* - Chronic daily dose via dermal absorption (mg/kg/d).

*C* - Pollutant concentration (mg/L).

The definitions and values of the other parameters used in the equations are listed in Table 2.

#### Risk characterization

Risk characterization integrates the data from hazard identification, dose-response, and exposure assessment to estimate the likelihood of adverse health effects from exposure to groundwater pollutants (Huang et al. 2018). It can be expressed as:

$$HI_{oral-water} = \frac{I_{CDI}}{RfD_{oral-water}} \quad (4)$$

$$HI_{derm-water} = \frac{I_{CDD}}{RfD_{derm-water}} \quad (5)$$

$$HI = HI_{oral-water} + HI_{derm-water} \quad (6)$$

Where:

*HI<sub>oral-water</sub>* - non-carcinogenic oral hazard coefficient (dimensionless).

**Table 2** Definitions and values of exposure assessment parameters

Parameter	Meaning	Value				Unit
		Children	Females	Males	Infants	
<i>EF</i>	Exposure frequency	365	365	365 <sup>b</sup>	365	d/a
<i>BW</i>	Average body weight	32.02 <sup>a</sup>	60.4 <sup>a</sup>	69.55 <sup>a</sup>	7.68 <sup>a</sup>	kg
<i>ABS</i>	Gastrointestinal absorption coefficient	0.5 <sup>c</sup>	0.5 <sup>c</sup>	0.5 <sup>c</sup>	0.5 <sup>c</sup>	
<i>IR</i>	Daily water intake	1.5 <sup>b</sup>	2 <sup>c</sup>	2 <sup>c</sup>	0.65 <sup>b</sup>	L/d
<i>ED</i>	Exposure duration	6 <sup>b</sup>	30 <sup>b</sup>	30 <sup>b</sup>	0.5 <sup>d</sup>	a
<i>SA</i>	Body surface areas	9035.2	1600 <sup>a</sup>	1700 <sup>a</sup>	3416	cm <sup>2</sup>
<i>AT</i>	Average exposure time	2190	10950	10950	182.5 <sup>b</sup>	d
<i>EV</i>	Bathing frequency	1 <sup>b</sup>				time/d
<i>ET</i>	Bath time	0.167 <sup>c</sup>				h/d
<i>CF</i>	Unit conversion factor	0.002 <sup>b</sup>				L/cm <sup>3</sup>
<i>KP</i>	Dermal adsorption	0.001 <sup>b</sup>				cm/h

a Data source: The State Council of the People's Republic of China (2021).

b Data source: Tian et al. (2020a).

c Data source: Sun et al. (2024c).

d Data source: Tian et al. (2020c).

e Data source: The National Bureau of Statistics of the People's Republic of China (2003).

$HI_{\text{derm-water}}$  - non-carcinogenic skin hazard coefficient (dimensionless).

$RfD_{\text{oral-water}}$  - reference dose of drinking water (mg/kg/d), 0.06 for  $F^-$ , and 0.001 for Cd.

$RfD_{\text{derm-water}}$  - reference dose absorbed by skin (mg/kg/d), 0.03 for  $F^-$ , and 0.0005 for Cd.

$HI$  - total risk index (dimensionless).

According to USEPA standards, an  $HI$  value less than 1 indicates an acceptable level of non-carcinogenic risk (Xu et al. 2023; Sun et al. 2022a, 2022b; Zhou et al. 2016; Ni et al. 2010).

To provide targeted protection strategies, this paper study assesses the health risks of  $F^-$  and Cd for four demographic groups: Infants ( $\leq 1$  year), children (2–17 years), adult males and adult females. The relevant exposure parameters for each group are provided in Table 2.

## 2 Results

### 2.1 Single indicator groundwater quality evaluation

The evaluation results of groundwater quality based on individual indicators are shown in Table 3 and Fig. 2.

As shown in Fig. 2, the overall groundwater quality in the study area is relatively good. Most indicators comply with Class I standards, and the majority of parameters fall within Class I to III ranges. Only four indicators exceeded Class V standards—turbidity pH,  $SO_4^{2-}$ ,  $F^-$ —each with an exceedance rate of 3% to 5%. Additionally, five indicators met Class IV standards, namely turbidity pH, Cd,  $CaCO_3$ ,  $F^-$ , with exceedance rates of

**Table 3** Single index evaluation results of groundwater quality

Indicator	Class I	Class II	Class III	Class IV	Class V
Colour	100%	0%	0%	0%	0%
Odor	100%	0%	0%	0%	0%
Turbidity	58%	0%	0%	37%	5%
Visible objects	100%	0%	0%	0%	0%
pH	87%	0%	0%	11%	3%
Al	0%	92%	8%	0%	0%
Mn	97%	0%	3%	0%	0%
Cu	100%	0%	0%	0%	0%
Zn	97%	3%	0%	0%	0%
$Cl^-$	100%	0%	0%	0%	0%
$SO_4^{2-}$	95%	3%	0%	0%	3%
$CaCO_3$	29%	66%	3%	3%	0%
TDS	79%	18%	3%	0%	0%
COD	87%	11%	3%	0%	0%
As	100%	0%	0%	0%	0%
Cd	92%	0%	0%	8%	0%
$Cr^{6+}$	82%	16%	3%	0%	0%
Pb	100%	0%	0%	0%	0%
Hg	100%	0%	0%	0%	0%
Se	100%	0%	0%	0%	0%
$F^-$	13%	68%	13%	3%	3%
$NO_3^-$	100%	0%	0%	0%	0%
$NH_4^+$	68%	0%	32%	0%	0%
$Na^+$	100%	0%	0%	0%	0%
$NO_2^-$	0%	92%	8%	0%	0%
Ni	100%	0%	0%	0%	0%

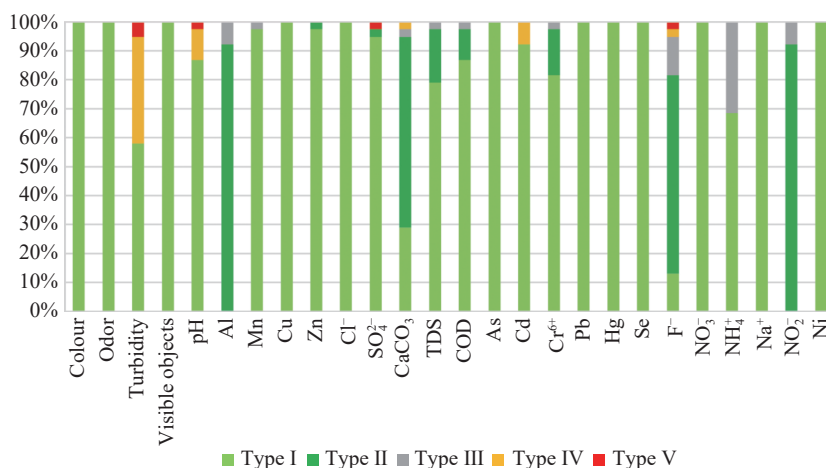


**Fig. 2** Stacked bar chart of single-indicator groundwater quality evaluation

37%, 11%, 8%, 3%, and 3%, respectively.

The evaluation results show that fluoride and cadmium exceed the thresholds set for safe drinking water, corresponding to Class V and Class IV, respectively. Therefore, the subsequent sections will focus on analysing the spatial distribution characteristics of F<sup>-</sup> and Cd and their potential health risks to local population.

## 2.2 Correlation analysis of substances in groundwater

The Pearson correlation coefficient matrix is a widely used tool in hydrogeochemical studies to quantitatively and intuitively express the correlation between various ions or indicators. In this study, the correlation coefficient matrix of water quality indicators was calculate using SPSS19 software, and the results are presented in Table 4.

From Table 4, it can be seen that:

CaCO<sub>3</sub> exhibits a strong positive correlation

with TDS, Ca<sup>2+</sup>, and Mg<sup>2+</sup> (correlation coefficients > 0.8), suggesting that these parameters are closely interrelated and likely share common geochemical origins. CaCO<sub>3</sub> is also moderately correlated with SO<sub>4</sub><sup>2-</sup> and Sr (0.6 < r < 0.8), indicating a secondary association with these ions.

TDS shows strong correlations with CaCO<sub>3</sub>, Ca<sup>2+</sup>, and Sr (all r > 0.8), and moderate correlations with SO<sub>4</sub><sup>2-</sup> and Mg<sup>2+</sup> (0.6 < r < 0.8). This indicates that the overall salinity of groundwater (as indicated by TDS) is largely controlled by these major ions.

Ca<sup>2+</sup> and SO<sub>4</sub><sup>2-</sup> are highly correlated (r = 0.884\*\*), suggesting a geochemical association such as gypsum (CaSO<sub>4</sub>·2H<sub>2</sub>O) dissolution or similar sources.

pH is negatively correlated with SO<sub>4</sub><sup>2-</sup>, Ca<sup>2+</sup>, Sr, and TDS, indicating that more acidic groundwater may favour the dissolution and release of these ions.

Sr shows strong positive correlations with Ca<sup>2+</sup>

**Table 4** Correlation matrix of groundwater hydrochemical parameters

	t.d	CaCO <sub>3</sub>	TDS	pH	Ca <sup>2+</sup>	Mg <sup>2+</sup>	SO <sub>4</sub> <sup>2-</sup>	F <sup>-</sup>	Cd	Sr
t.d	1									
CaCO <sub>3</sub>	-0.072	1								
TDS	-0.06	0.990**	1							
pH	-0.108	-0.322	-0.371*	1						
Ca <sup>2+</sup>	0.01	0.931**	0.962**	-0.505**	1					
Mg <sup>2+</sup>	-0.122	0.840**	0.779**	0.018	0.593**	1				
SO <sub>4</sub> <sup>2-</sup>	-0.034	0.734**	0.785**	-0.596**	0.884**	0.354	1			
F <sup>-</sup>	0.032	-0.034	-0.013	-0.046	0.088	-0.192	0.224	1		
Cd	-0.016	0.137	0.082	0.307	-0.009	0.25	-0.067	-0.168	1	
Sr	-0.002	0.795**	0.835**	-0.570**	0.914**	0.412*	0.953**	0.237	0.085	1

Notes: \*\* At the 0.01 level (bilateral), there is a significant correlation.

\* At the 0.05 level (bilateral), there is a significant correlation.

t.d- turbidity degree.

TDS- Total Dissolved Solids.

and  $\text{SO}_4^{2-}$ , reflecting its similar geochemical behaviour due to its group association with calcium and similar solubility patterns in aquifers.

$\text{F}^-$  displays very weak or no correlation with any other indicator. The highest correlation observed is with Sr ( $r = 0.237$ ), followed by  $\text{SO}_4^{2-}$  ( $r = 0.224$ ), both indicating only weak associations. The correlations with all other parameters are below 0.2, signifying very weak or negligible relationships. This suggests that fluoride likely originates from distinct geochemical processes or sources, independent of major ions.

Cd also exhibits weak correlations with other parameters, with its strongest correlation being with pH ( $r = 0.307$ ), followed by  $\text{Mg}^{2+}$  ( $r = 0.250$ ). All other correlations are below 0.2, indicating limited or no association with the rest of the hydrochemical parameters. This may imply point-source pollution or localized geogenic enrichment.

Both  $\text{F}^-$  and Cd show weak or no correlation with most other indicators, indicating that they likely have independent sources or mobilization mechanisms compared to the major ions in the groundwater system.

### 2.3 Spatial distribution characteristics of $\text{F}^-$ and Cd in groundwater

The fluoride ( $\text{F}^-$ ) concentrations in groundwater within the study area range from 0.16 mg/L to 2.70 mg/L, with an average value of 0.42 mg/L. In most parts of the region, the groundwater quality with respect to  $\text{F}^-$  corresponds to Class I to III water standards, indicating low to moderate concentrations. Such water is generally suitable for various uses, including centralized domestic, industrial, and agricultural water uses.

However, in the eastern portion of the study area, groundwater with Class IV quality level is observed, characterized by high  $\text{F}^-$  concentrations. According to water quality standards for agricultural and industrial water uses and considering potential human health risks, this water is suitable primarily for agricultural and some industrial purposes and can be used as drinking water after appropriate treatment. More critically, areas with Class V water also located in the east side of the study area, show high  $\text{F}^-$  concentrations that render the groundwater unsuitable for domestic water supply. In this case, alternative water sources should be selected for various uses. The extent of fluoride exceedance in the area is quite serious, suggesting potential health risks that warrant detailed assessment, as shown in Fig. 3.

Cadmium (Cd) concentrations in the groundwa-

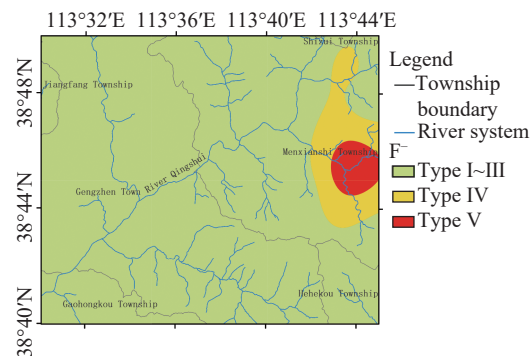


Fig. 3 Spatial distribution map of  $\text{F}^-$

ter range from 0.0001 mg/L to 0.0079 mg/L, with an average value of 0.0007 mg/L. Most of the region exhibits Class I to III water quality for Cd, reflecting low to moderate chemical content levels suitable for a wide range of uses, including centralized drinking water sources and industrial and agricultural water uses. Class IV water appears in the west and northwest of the study area, specifically in the central northern and southern parts of Gengzhen Town, and the northwestern area of Menxianshi Township. Elevated Cd concentrations imply that groundwater is more suitable for agricultural and industrial uses, and can be considered for drinking water after appropriate treatment. Direct consumption without treatment may pose health risks, necessitating further evaluation through health risk assessment, as shown in Fig. 4.

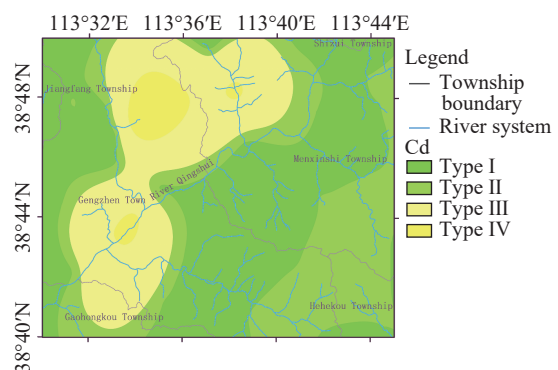
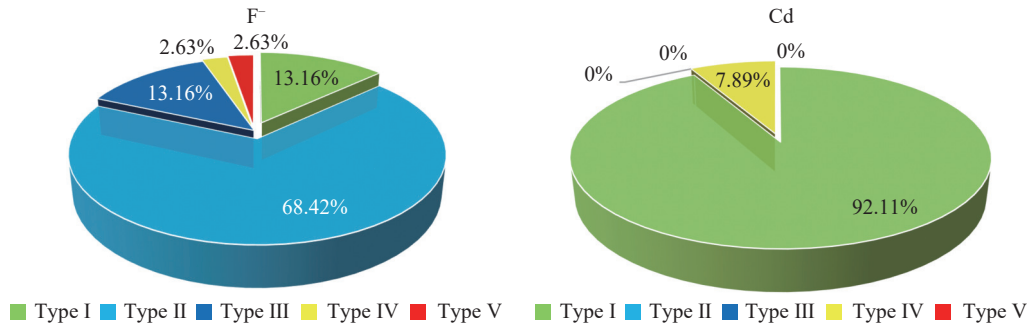


Fig. 4 Spatial distribution map of Cd

The proportions of groundwater classified by  $\text{F}^-$  water quality classes I, II, III, IV, and V are 13.16%, 68.42%, 13.16%, 2.63%, and 2.63%, respectively. For Cd, the corresponding proportions for classes I, II, III, IV, and V are 92.11%, 0.00, 0.00, 7.89%, and 0.00 respectively, as illustrated in Fig. 5.

### 2.4 Health risk assessment

According to the evaluation results, no significant health risk is associated with Cadmium (Cd), as the



**Fig. 5** Proportion of  $F^-$  and Cd in various types of water

Hazard Index (HI) values are all below 1 (Table 5). Conversely, Fluoride ( $F^-$ ) poses a health risk since its HI values exceed 1 (Table 6).

To visualize the spatial distribution of health risks from fluoride enrichment, a health risk assessment map was created (Fig. 6). This map reveals that  $F^-$ -related health risks are primarily concentrated in the eastern part of the study area, corresponding to Menxianshi Township.

The results indicate that the  $F^-$  in groundwater poses a risk to adult male only in a small area in eastern Menxianshi Township, Wutai County (Fig. 6a). For adult females, the risk index is higher than that for adult males ( $HI > 1$ ), with the risk zone also located in eastern Menxianshi Township (Fig. 6b). This gender disparity aligns with findings from the Weining Plain in northwest China, highlighting the importance of considering gender differ-

**Table 5** Statistical summary of hazard coefficient for Cd

Group	Males	Females	Children	Infants
$HI_{\text{derm-water}}$	0.0008	0.0008	0.0089	0.0066
$HI_{\text{oral-water}}$	0.2272	0.2616	0.3701	0.6686
HI	0.2279	0.2624	0.3790	0.6752

**Table 6** Statistical summary of hazard coefficient of  $F^-$

Group	Males	Females	Children	Infants
$HI_{\text{derm-water}}$	0.004	0.005	0.051	0.037
$HI_{\text{oral-water}}$	1.293	1.489	2.106	3.806
HI	1.297	1.494	2.157	3.843

ences in HHRA. Risk indices for children and infants are significantly higher than those for

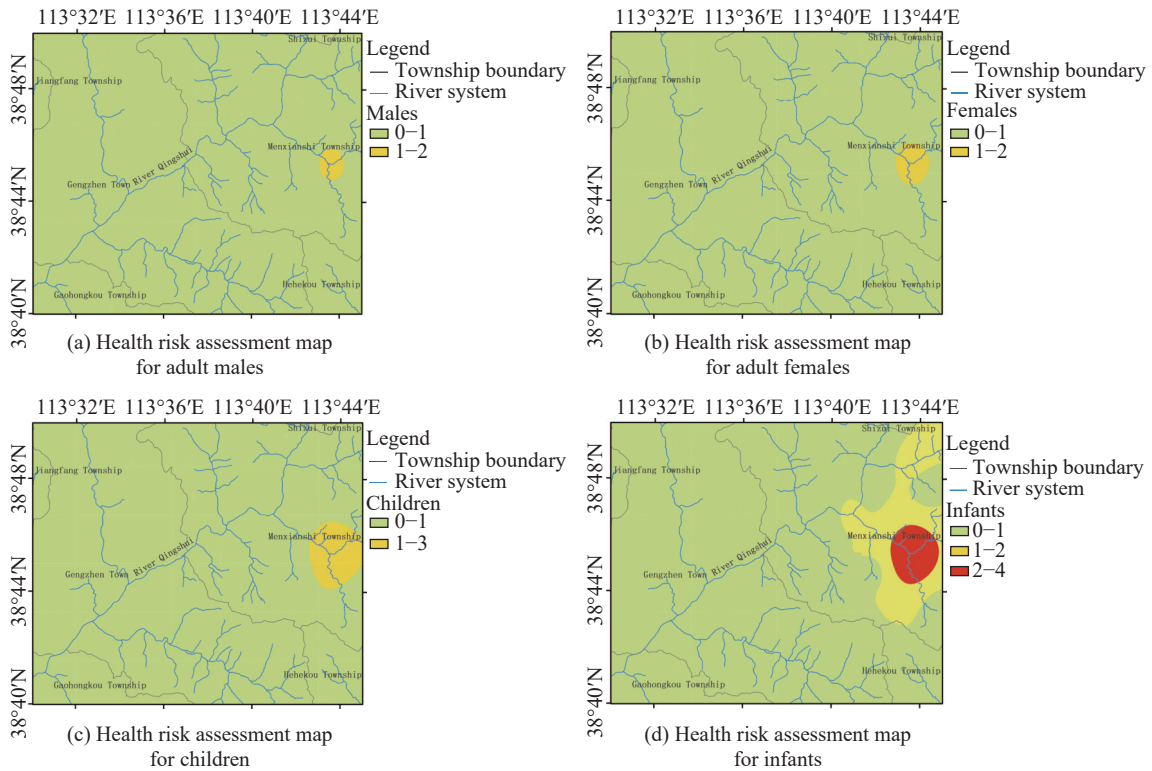


**Fig. 6** Health risk assessment map for infants

adults, with the maximum HI values reaching 2.16 for children (Fig. 6c) and 3.86 for infants (Fig. 6d), mainly distributed in the eastern region.

The overall HHRA results are shown in Fig. 7. The maximum HI value for adult males is 1.30, with an average of 0.19; The maximum HI value for adult females is 1.49, with an average of 0.22; The maximum HI value for children is 2.16, with an average of 0.32; The maximum HI value for infants is 3.84, with an average of 0.58. These results indicate a clear gradient in health risks: Infants>children>adult females>adult males. The higher risks among females compared to males is mainly attributed to differences in body weight across demographic groups.

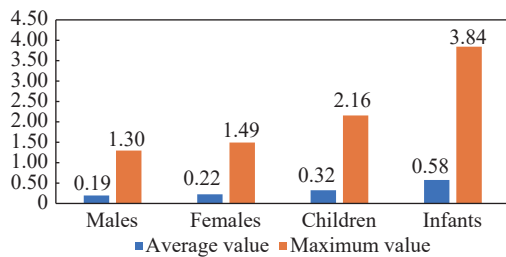


Fig. 7 Risk bar chart for different age and gender groups

The comparative analysis of exposure routes (drinking water intake versus dermal absorption) is presented in Fig. 8. Health risks from drinking water ingestion are significantly higher than those from dermal contact. Specifically, the HI values of ingestion for adult males, adult females, children, and infants are 1.293, 1.489, 2.106, and 3.806, respectively, while dermal exposure HI values are much lower, at 0.004, 0.005, 0.051, and 0.037, respectively. This indicates that ingestion of contaminated groundwater is the main exposure pathway responsible for health risks.

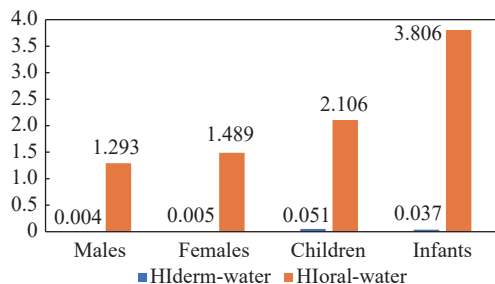


Fig. 8 Comparison of health risks by population group and exposure route

### 3 Discussion

The overall groundwater quality in Gengzhen

Town is good; however, certain substances exceed the standards for healthy drinking water. In response to the exceedance of hazardous substances such as fluoride (F<sup>-</sup>), a health risk assessment was conducted.

#### 3.1 Origin of fluoride (F<sup>-</sup>) enrichment

The fluoride enrichment zones are primarily concentrated in localized areas in the eastern part of the study area, with fluoride levels reaching Class V standards. The area is underlain predominantly by Precambrian metamorphic rock formations, within which fluoride-bearing minerals such as fluorite and fluorapatite were formed through magmatic activity and metamorphism. During weathering process, fluoride is released from these minerals and enters the aquifer with fissure water, especially along the contact zones between gneiss and marble formations. The presence of mineralized joints promotes the dissolution and mobilization of fluoride, providing a geochemical basis for its enrichment in groundwater. Hence, the release of F<sup>-</sup> from geological minerals is the fundamental cause of fluoride accumulation. Climatically, Gengzhen experiences a semi-arid temperate continental climate, with an annual precipitation ranging from 450 mm to 550 mm, contrasted by a much higher evaporation of 1,200–1,500 mm. The arid environment leads to slow groundwater recharge and runoff, promoting the concentration and accumulation of fluoride in the aquifer through evaporation processes (Yuan et al. 2024; Pan et al. 2013).

In summary, the elevated fluoride concentrations in Gengzhen's groundwater is the result of the combined effects of geological fluoride release and hydrological cycling under arid climatic conditions. Subsequent prevention and control measures should integrate geological surveying and hydrodynamic dynamic monitoring to intercept and manage the migration pathways of fluoride from its source.

#### 3.2 Health risks of F<sup>-</sup> enrichment in groundwater

Fluoride enrichment poses notable health risks in the study area. Based on the research results, the fluoride-related high-risk zones correspond spatially to F<sup>-</sup> enriched areas, mainly in the eastern part of the region. Although the high-risk areas are limited in extent, they warrant serious attention. Significant variability exists in the health

risks across different population groups. The risk indices for infants (3.843), children (2.157), adult females (1.494), and adult males (1.297) follow a decreasing trend, reflecting differences in physiological characteristics and exposure patterns.

Infants exhibit the highest risk index (3.843), attributable to their metabolic characteristics. The daily water intake of infants, calculated based on body weight ratio (approximately 150 mL/kg·d), is much higher than that of adults, while their renal capacity to excrete F<sup>-</sup> remains immature, resulting in enhanced bioaccumulation of fluoride in their body (Saravanan et al. 2022c).

Children's risk index (2.157) ranks second, mainly influenced by their vulnerability during critical growth phases. Children aged 6–12 undergo mineralization of permanent teeth, during which F<sup>-</sup> easily combines with enamel hydroxyapatite to form fluorapatite, potentially leading to enamel hypoplasia or fluorosis (Li et al. 2024).

Adult females have a higher risk (1.49) than males (1.297), which is related to physiological metabolism and calcium demands. The peak bone density of women is lower than that of men, and the demand for calcium increases during pregnancy and lactation. Fluoride's interaction with calcium can disrupt bone metabolism. In addition, post-menopause estrogen levels decrease and bone turnover rate accelerates, further increasing the fluoride-induced osteoporosis risk (Jing et al. 2022).

These population-specific risk differences indicate the need for precise prevention and control measures. Risk management should prioritize the most vulnerable groups in the order of "infants > children > adults", applying differentiated regulatory standards. Furthermore, integrating fluoride adsorption technologies and establishing dynamic monitoring networks can effectively mitigate exposure risks at the source.

## 4 Conclusion

Through the evaluation of groundwater quality, it was found that Fluoride (F<sup>-</sup>) and Cadmium (Cd) levels exceed drinking water standards in the study area. Fluoride concentrations reach Class V water quality standard, with enrichment primarily distributed in the eastern part of the study area. Cadmium levels meet the Class IV standards, with enrichment mainly distributed in the western and northwestern regions. In response to the excessive F<sup>-</sup> and Cd levels, a Groundwater Health Risk Model (HHRA) model was developed to effec-

tively evaluate their associated health risks. Although cadmium concentrations in groundwater slightly exceed the standard, they remain below the threshold for significant health risk. In contrast, fluoride enrichment in groundwater poses tangible health risks. Notably, health risks from fluoride contamination vary significantly differences among different genders and age groups, with risk ranking in the order of infants > children > adult females > adult males. Infants are the most vulnerable population, while adults exhibit stronger resilience against fluoride exposure compared to children and infants. It is recommended to scientifically treat water sources with health risks to ensure safe and healthy drinking water for the population.

## Acknowledgements

This research was supported by the Northeast Geological Science and Technology Innovation Center of China Geological Survey (Grant No. QCJJ2022-43), the Natural Resources Comprehensive Survey Project (Grant Nos. DD20230470, DD20230508), and the National Groundwater Monitoring Network Operation and Maintenance Program (Grant No. DD20251300109).

## References

- Alireza RD, Seyed AH, Vahid, et al. 2020. Assessing pollution risk in Ardabil aquifer groundwater of Iran with arsenic and nitrate using the SINTACS model. *Polish Journal of Environmental Studies*, 29: 2609. DOI: [10.15244/pjoes/112903](https://doi.org/10.15244/pjoes/112903).
- Anju M, Kavita. 2022. Fluoride contamination in groundwater of intensively cropped Upper Yamuna alluvial basin of India: A hydrogeochemical, human health risk assessment, and multivariate statistical perspective. *Arabian Journal of Geosciences*, 15: 1473. DOI: [10.1007/s12517-022-10728-9](https://doi.org/10.1007/s12517-022-10728-9).
- Cao W, Fu Y, Cheng Y, et al. 2023a. Modeling potential arsenic enrichment and distribution using stacking ensemble learning in the lower Yellow River Plain, China. *Journal of Hydrology*, 625: 129985. DOI: [10.1016/j.jhydrol.2023.129985](https://doi.org/10.1016/j.jhydrol.2023.129985).
- Cao W, Zhang Z, Fu Y, et al. 2024 Prediction of arsenic and fluoride in groundwater of the

- North China Plain using enhanced stacking ensemble learning. *Water Research*, 259: 121848. DOI: [10.1016/j.watres.2024.121848](https://doi.org/10.1016/j.watres.2024.121848)
- Cao W, Zhang Z, Guo H, et al. 2023b. Spatial distribution and controlling mechanisms of high fluoride groundwater in the coastal plain of Bohai Rim, North China. *Journal of Hydrology*, 617: 128952. DOI: [10.1016/j.jhydrol.2022.128952](https://doi.org/10.1016/j.jhydrol.2022.128952).
- Chen J, Wu H, Qian, H, et al. 2017. Assessing nitrate and fluoride contaminants in drinking water and their health risk of rural residents living in a semiarid region of northwest China. *Exposure and Health*, 9: 183. DOI: [10.1007/s12403-016-0231-9](https://doi.org/10.1007/s12403-016-0231-9).
- Churchill HV, Rowley RJ, Martin LN. 1948. Flourine content of certain vegetation in western Pennsylvania area. *Analytical Chemistry*, 20(1): 69–71. DOI: [10.1021/ac60013a018](https://doi.org/10.1021/ac60013a018).
- Huang Y, Zuo, R, Li J, et al. 2018. The spatial and temporal variability of groundwater vulnerability and human health risk in the Limin District, Harbin, China. *Water*, 10: 686. DOI: [10.3390/w10060686](https://doi.org/10.3390/w10060686).
- Hu Q, Guo QL, Yang YS, et al. 2024. Analysis on characteristics and sources of heavy metal pollution in groundwater in coal mining areas. *Nonferrous Metals (Extractive Metallurgy)*, (4): 111–119,177. DOI: [10.3390/w15234091](https://doi.org/10.3390/w15234091).
- Jing XY, Li XZ, Wang WJ, et al. 2022. Distribution characteristics and health risk assessment of fluorine in groundwater in Yinchuan Plain. *Environmental Science & Technology*, 45(2): 174–181. (in Chinese). DOI: [10.19672/j.cnki.1003-6504.1833.21.338](https://doi.org/10.19672/j.cnki.1003-6504.1833.21.338).
- José RR, Carlos R, Lawren E, et al. 2021. Russell Flegal. Monitoring of As, Cd, Cr, and Pb in groundwater of Mexico's agriculture Mocerito River aquifer: Implications for risks to human health. *Water, Air, Soil Pollution*, 232(7): 1–20. DOI: [10.1007/s11270-021-05238-5](https://doi.org/10.1007/s11270-021-05238-5).
- Li FY, Jiang TY, Yu T, et al. 2021. Review on sources of fluorine in the environment and health risk assessment. *Rock and Mineral Analysis*, 40(6): 793–807. (in Chinese). DOI: [10.15898/j.cnki.11-2131/td.202109290133](https://doi.org/10.15898/j.cnki.11-2131/td.202109290133).
- Li XZ, Cao WG, Li Y, et al. 2024. The hazards of fluorine-containing groundwater, current status and progress of treatment technologies. *Geology in China*, 51(2): 457–482. (in Chinese). DOI: [10.12029/gc20230513001](https://doi.org/10.12029/gc20230513001).
- Li ZX, Gui HQ. 1980. Fluorine pollution and its enrichment in groundwater in Baotou area. *Hydrogeology and Engineering Geology*, 7(4): 49–50. (in Chinese).
- Marghade D, Malpe DB, SubbaRao N. 2021. Applications of geochemical and multivariate statistical approaches for the evaluation of groundwater quality and human health risks in a semi-arid region of eastern Maharashtra, India. *Environmental Geochemistry and Health*, 43: 683. DOI: [10.1007/s10653-019-00478-1](https://doi.org/10.1007/s10653-019-00478-1).
- Ni B, Wang HB, Li XD, et al. 2010. Environmental health risk assessment of drinking water source in lakes. *Environmental Science and Pollution Research*, 46(1): 74–79. (in Chinese). DOI: [10.13198/j.res.2010.01.76.nib.012](https://doi.org/10.13198/j.res.2010.01.76.nib.012).
- Nitika M, Anju M, Shewane B. 2021. Assessment of groundwater hydro-geochemistry, quality, and human health risk in arid area of India using chemometric approach. *Arabian Journal of Geosciences*, 14: 1546. DOI: [10.1007/s12517-021-07852-3](https://doi.org/10.1007/s12517-021-07852-3).
- Pan YL, Su CL, Wang YX, et al. 2013. Distribution characteristics and controlling factors of fluoride in sediments in the Shanyin Yingxian area of Datong Basin. *Mineral Rocks*, 33(02): 109–114. (in Chinese). DOI: [10.19719/j.cnki.1001-6872.2013.02.015](https://doi.org/10.19719/j.cnki.1001-6872.2013.02.015).
- Sanjay P, Bhavesh P, Ajaykumar K, et al. 2024. Nitrate and fluoride contamination in the groundwater in a tribal region of north Maharashtra, India: An account of health risks and anthropogenic influence. *Groundwater for Sustainable Development*, 25: 101107. DOI: [10.1016/j.gsd.2024.101107](https://doi.org/10.1016/j.gsd.2024.101107).
- Saravanan R, Balamurugan P, Shunmuga PK. 2022. Effect of high nitrate contamination of groundwater on human health and water qual-

- ity index in semi-arid region, south India. *Arabian Journal of Geosciences*, 15: 242. DOI: [10.1007/s12517-022-09553-x](https://doi.org/10.1007/s12517-022-09553-x).
- State Council of the People's Republic of China, Report on the nutrition and chronic disease status of Chinese Residents, 2021.
- Sun QF, Sun ZA, Tian H. et al. 2020a. Dynamic characteristics and difference analysis of the groundwater in Changchun New District. *Geology and Resources*, 29: 369. (in Chinese). DOI: [10.13686/j.cnki.dzyzy.2020.04.010](https://doi.org/10.13686/j.cnki.dzyzy.2020.04.010).
- Sun QF, Jia LG, Tian H, et al. 2020b. Chemical characteristics and genesis analysis of the groundwater in Lianhuashan Area, Changchun City. *Geology and Resources*, 29: 476. (in Chinese). DOI: [10.13686/j.cnki.dzyzy.2020.05.010](https://doi.org/10.13686/j.cnki.dzyzy.2020.05.010).
- Sun QF, Jia LG, Sun ZA, et al. 2022a. Characteristics and applicability of groundwater quality in Oroqen Qi, Inner Mongolia. *Geology and Resources*, 31: 88. (in Chinese). DOI: [10.13686/j.cnki.dzyzy.2022.01.011](https://doi.org/10.13686/j.cnki.dzyzy.2022.01.011).
- Sun QF, Yang K, Sun ZA, et al. 2022b. Characteristics of groundwater quality in Changchun new area and its evaluation on ecological health. *Geology in China*, 49: 834. (in Chinese). DOI: [10.12029/gc20220311](https://doi.org/10.12029/gc20220311).
- Sun QF, Sun ZA, Jia LG, et al. 2023a. Formation mechanism of strontiumrich and metasilicic acid groundwater in the Lianhuashan area, Changchun, Jilin Province. *Geology in China*, 50(1): 181–190. (in Chinese). DOI: [10.12029/gc20200624001](https://doi.org/10.12029/gc20200624001).
- Sun QF, Yang K, Liu T, et al. 2023b. Health risk assessment of nitrate pollution of drinking groundwater in rural areas of Suihua, China. *Journal of Water and Health*, 21(9): 1193–1208. DOI: [10.2166/wh.2023.069](https://doi.org/10.2166/wh.2023.069).
- Sun QF, Lang GH, Liu T, et al. 2024a. Health risk analysis of nitrate in groundwater in Shanxi Province, China: A case study of the Datong Basin. *Journal of Water and Health*, 22(4): 701–716. DOI: [10.2166/wh.2024.320](https://doi.org/10.2166/wh.2024.320).
- Sun QF, Yang K, Li CH, et al. 2024b. Analysis on the chemical characteristics and genesis of drinking groundwater in rural areas of Suihua City, Northeast China. *Environmental Forensics*, 1–12. DOI: [10.1080/15275922.2023.2297871](https://doi.org/10.1080/15275922.2023.2297871).
- Sun QF, Guo L, Hu C, et al. 2024c. Health risk assessment of drinking groundwater in rural areas of Ru village and surrounding areas in Wutai County, China. *Journal of Water and Health*, 22(1): 183–196. DOI: [10.2166/wh.2023.277](https://doi.org/10.2166/wh.2023.277).
- Tian H, Du JZ, Sun QF, et al. 2020a. Using the Water Quality Index (WQI), and the Synthetic Pollution Index (SPI) to evaluate the groundwater quality for drinking purpose in Hailun, China. *Sains Malaysiana*, 49: 2383. DOI: [10.17576/jsm-2020-4910-05](https://doi.org/10.17576/jsm-2020-4910-05).
- Tian H, Sun QF, Kang Z, et al. 2020b. Groundwater chemistry and health risks associated with nitrate intake in Hailun, Northeast China. *Journal of Water and Health*, 18: 1033. DOI: [10.2166/wh.2020.050](https://doi.org/10.2166/wh.2020.050).
- Tian H, Liang XJ, Gong Y, et al. 2020c. Risk assessment of metals from shallow groundwater in Lianhuashan District, China. *La Houille Blanche*, 119: 5. DOI: [10.1051/lhb/2019063](https://doi.org/10.1051/lhb/2019063).
- Tian H, Liang XJ, Gong Y, et al. 2020d. Health risk assessment of nitrate pollution in shallow groundwater: A case study in China. *Polish Journal of Environmental Studies*, 29: 827. DOI: [10.1051/lhb/2019055](https://doi.org/10.1051/lhb/2019055).
- USEPA. 2001. Risk assessment guidance for superfund Volume III: Part A, Process for conducting probabilistic risk assessment. US Environmental Protection Agency, Washington, DC, USA.
- Xiao J, Jin ZD, Zhang F. 2015. Geochemical controls on fluoride concentrations in natural waters from the middle Loess Plateau, China. *Journal of Geochemical Exploration*, 159: 252–261. DOI: [10.1016/j.gexplo.2015.09.018](https://doi.org/10.1016/j.gexplo.2015.09.018).
- Xu JJ, Zhao YL, Chen HY, et al. 2023. ABC-GSPBFT: PBFT with grouping score mechanism and optimized consensus process for flight operation data-sharing. *Information Sciences*, 624: 110–127. DOI: [10.1016/j.ins](https://doi.org/10.1016/j.ins).

2022.12.068.

Yuan TJ, Jin G, Li YF, et al. 2024. Analysis of the sources and enrichment mechanisms of fluoride in the groundwater system of Datong Basin. *Safety and Environmental Engineering*, DOI:10.13578/j.cnki.issn.1671-1556.

20240139.

Zhou YH, Wei AH, Li JF, et al. 2016. Groundwater quality evaluation and health risk assessment in the Yinchuan Region, Northwest China. *Exposure and Health*, 8: 443. DOI: 10.1007/s12403-016-0219-5.